Applied Physics Express

LETTER

Liquid photoacoustic sensing with high sensitivity by temperature compensated differential detection method

Applied Physics Express 13, 117001 (2020)
https://doi.org/10.35848/1882-0786/abbd26

LETTER

Liquid photoacoustic sensing with high sensitivity by temperature compensated differential detection method

Qiaozhi He, Qian Wang, Pengfei Lv, Zhiqian Lu, Na Lv, Hui Zhao*, and Wei Tao*

Department of Instrument Science and Engineering, Shanghai Jiao Tong University, 200240 People's Republic of China

*E-mail: huizhao@sjtu.edu.cn; taowei@sjtu.edu.cn

Received September 15, 2020; revised September 27, 2020; accepted September 30, 2020; published online October 15, 2020

In this letter, a temperature compensated differential (TCD) photoacoustic (PA) method is proposed to simultaneously suppress the side-effect of multiple interferences, significantly improving the accuracy and sensitivity of liquid PA detection. We firstly established a theoretical model to prove the validity of this method. Then a differential PA detection system was set up to detect glucose concentration, a typical weak absorbing substance in the near-infrared range. The experimental results demonstrate that a trace-level detection limit of 9.95 mg dl^{-1} (99.5 ppb) for glucose solution was obtained. The TCD-PA method provides a feasible way for on-line high-precision detection of liquid substances.

On-line liquid substance detection with trace-level accuracy is challenging due to the balance of detection accuracy and portability[1]. Currently, the mainstream methods for liquid substance detection include chemical titration method,[2] inductively coupled plasma-mass spectrometry (ICP-MS)[3] as well as similar methods,[4] and optical detection methods. The chemical titration method relies on pipetting and observational accuracy, the precision of which is hard to guarantee.[5] ICP-MS requires the medium ionization of liquids at ultra-high temperatures (above 2300 °C),[6] which is difficult to meet the requirements of on-line liquid detection due to the demanding detection environment and complex sample pretreatment.[7] Optical detection methods are one of the most promising methods for high-precision on-line detection of liquid substances.[8] Such methods perform non-destructive detection, mainly including absorption spectroscopy (AS),[9] fluorescence spectroscopy,[10] Raman spectroscopy[11] and photoacoustic (PA) spectroscopy.[12] AS method is essential to detect the proportion of light transmission, which is not sensitive to strong and weak absorption substances.[13] Fluorescence spectroscopy and Raman spectroscopy have special demands for the optical properties of the test substance, such as the fluorescence excitation property and strong scattering property.[14,15] The PA spectroscopy is an emerging detection method converting light energy into acoustic energy,[16] which is widely applied in substance sensing and biological imaging.[17] The detection accuracy can be easily improved by increasing the laser energy, which is more suitable for high-precision detection than AS.[18] We previously used PA and AS method to detect mercury ion in aqueous solution, which demonstrated that the PA method has a much lower detection limit (78 pM)[19] compared to the AS method (37 nM).[20]

In recent years, gas and solid PA detection has developed rapidly and widely used in the high-precision detection field,[21] whereas the development of liquid PA detection is sluggish. The sound transmission medium for liquid PA detection changes from gas to liquid, making thermal expansivity decrease dramatically.[22,23] Only weak liquid PA signals can be obtained, then the intensity of which is about two orders of magnitude weaker than gas or solid. The two main detection modes for PA detection are CW laser-microphone-lockin amplifier[24] and pulsed laser-piezoelectric transducer-electric amplifier.[25] Due to low natural frequency (less than 10 Hz), gas PA detection generally applies the former detection mode. In contrast, the natural frequency of liquid ranges from 10 to 400 kHz.[26] The modulation frequency of continuous laser and the working frequency of lock-in amplifiers can hardly reach high frequency over MHz level, thus the latter detection mode works for liquid PA detection.[27] Currently, the output laser intensity of high-power pulsed lasers is unstable, which directly affects the detection accuracy of PA detection. Besides, the external electromagnetic, acoustic interference and temperature fluctuations can also affect the PA signals. The above reasons make the accuracy of liquid PA detection difficult to meet the high-precision sensing requirement.[28]

In this letter, a temperature compensated differential PA detection (TCD-PA) method is proposed to address the above challenge. The TCD-PA method combines temperature compensation (TC) and differential PA method, which effectively suppresses laser intensity fluctuation and other multiplicative environmental interference, enhance the stability of the PA signal, and finally achieve trace-level liquid PA detection.

Based on the Beer–Lambert law, the relationship between the incident intensity I_A and absorption intensity I_0 is:[29]

$$\begin{aligned} I_A &= I_0 - I_0 \exp(-N_0\sigma_0 L - N_s\sigma_s L) \\ &= I_0 - I_0 \exp\left(-N_0\sigma_0 L\left(1 + \frac{\sigma_s}{\sigma_0 N_0}N_s\right)\right), \end{aligned} \quad (1)$$

where N_0 and N_s represent the molecular number density (cm^{-3}) of the solvent and solute; σ_0 and σ_s are the effective absorption cross-section area (cm^{-2}), which are independent with concentration; L is the optical path length (cm) of light through the entire solution. For most solutions, such as the glucose solution, the absorption of the entire liquid is very weak in visible and near-infrared bands. Thus, Eq. (1) can be approximated by Taylor series as $I_A = I_0 - I_0[1 - N_0\sigma_0 L(1 + KN_s)] = N_0\sigma_0 L(1 + KN_s)I_0$, where $K = \sigma_s/\sigma_0 N_0$, K and N_0 can be taken as a constant since the content of solvent is much larger than the content of solute.

To improve the efficiency of PA conversion in liquid, the laser energy used in liquid PA measurement is usually short-pulse and high-energy laser. The intensity of the incident laser can be written as Eq. (2)

$$I_0 = E_0 f(t) g(\vec{r}) = \frac{E_0}{(2\pi)^{3/2}\tau_p R^2} \exp\left(-\frac{t^2}{2\tau_p^2} - \frac{r^2}{2R^2}\right), \quad (2)$$

where E_0 is the total energy of single pulse, τ_p is the time at which the light intensity drops from the strongest intensity to

$1/e^2$, R is the laser beam radius. The two profiles f and g are normalized as $\int f(t)dt = 1$ and $\int g(\vec{r})d^2\vec{r} = 1$.

After absorption, the liquid immediately expands and contracts, exciting a PA wave. A PA wave completely disappears within a few microseconds. With the thermodynamic wave equation, we can approximate the fluid motion as linear and use the expression of the PA wave as Eq. (3). In the derivation, the thermal diffusion is ignored, since it usually takes much longer time

$$\left(\frac{1}{\upsilon^2}\frac{\partial^2}{\partial t^2} - \nabla^2\right)P_A = \frac{\beta}{C_p}\frac{\partial I_A}{\partial t}, \tag{3}$$

where υ, β, C_p are the acoustic velocity, volume expansivity and specific heat at constant pressure, respectively. To simplify the derivation, a new parameter Φ is introduced,[30] which is shown in Eq. (4)

$$\left(\frac{1}{\upsilon^2}\frac{\partial^2}{\partial t^2} - \nabla^2\right)\Phi = I_0. \tag{4}$$

Then, the excess pressure P_A of PA wave can be expressed as $P_A = \frac{\beta}{C_p}N_0\sigma_0 L(1 + KN_s)\frac{\partial\Phi}{\partial t}$, where $K = \frac{\sigma_s}{\sigma_0 N_0}$. To solve a partial differential equation like Eq. (4), a Green's function is designed to simplify the derivation, which is shown in Eq. (5)

$$\left(\frac{1}{\upsilon^2}\frac{\partial^2}{\partial t^2} - \nabla^2\right)G(t, \vec{r}) = \sigma(t - t')\sigma(\vec{x} - \vec{x'}), \tag{5}$$

where $G(t, \vec{x})$ is the designed Green's function, $\vec{x} = (x, y, z)$ and $\vec{x'} = (x', y', z')$. Equation (5) can be converted to a inhomogeneous form of Helmholtz equation by using Fourier transform as $\nabla^2 G_\omega + \frac{\omega^2}{\upsilon^2}G_\omega = \sigma(\vec{x} - \vec{x'})$. Since the source of PA wave is the liquid located in the light path, the PA wave spreads out in a cylindrical shape. Equation (5) is transformed to cylindrical inhomogeneous Helmholtz equation as Eq. (6) shows, where we suppose the angular and altitude components keep identical at different position

$$\frac{1}{r}\frac{\partial}{\partial r}\left(r\frac{\partial G_\omega}{\partial r}\right) + \frac{\omega^2}{\upsilon^2}G_\omega = -\frac{\sigma(r - r')}{\pi(r - r')}. \tag{6}$$

To further simplify Eq. (6), a Hankel transform of zero order, $G_{\omega\kappa}(\kappa) = \int_0^\infty G_\omega(r)J_0(\kappa r)\kappa dr$, is applied, where κ is wave number. The simplest form of Eq. (6) is $G_{\omega\kappa} = \frac{2}{\kappa^2 - k_0^2}$, where $k_0 = \omega/\upsilon$. After inverse Fourier transform and inverse Hankel transform of zero, the Green's function is explicitly solved.

$$\begin{aligned} G(t, \vec{r}) &= 2\upsilon\Theta(t)\int_0^\infty \frac{\sin(\upsilon\kappa t)}{\kappa}J_0(\kappa r)\kappa d\kappa, \\ &= \Theta(t)\frac{2\upsilon}{\sqrt{(\upsilon t)^2 - r^2}} \end{aligned} \tag{7}$$

where $\Theta(t)$ is the unit step function.

For the Gaussian time profile and Gaussian radial profile, Φ can be further reduced and solved as Eq. (8)

$$\begin{aligned} \Phi(t, \vec{r}) &= \frac{E_0}{r}\int\int G(t - t', \vec{r} - \vec{r'})f(t')g(\vec{r'})d^2\vec{r'}dt' \\ &= \frac{E_0\upsilon}{8R\sqrt{\pi r}}\sqrt{t}\left[\frac{\sqrt{2}}{\pi}K_{1/4}\left(\frac{t^2}{4\tau_e^2}\right)\right. \\ &\quad \left. + 2I_{1/4}\left(\frac{t^2}{4\tau_e^2}\right)\right]\exp\left(\frac{t^2}{4\tau_e^2}\right), \end{aligned} \tag{8}$$

where $\tau_e^2 = \tau_p^2 + \frac{R^2}{\upsilon^2}$, introduced by Lai and Young.[30] For Nd:YAG solid-state laser, τ_p is normally less than 10 ns, whereas R is normally around 0.5 mm. The acoustic velocity of water at room temperature is around 1500 m s^{-1}.[31] Therefore, $\tau_p \ll \frac{R}{\upsilon}$, i.e. $\tau_e \approx \frac{R}{\upsilon}$. I and K are the modified Bessel function of the first kind and second kind.

In the proposed differential PA measurement method, the measured parameter is the amplitude of PA signals generated from the test solution and reference solution. The time profile $\frac{d\Phi}{dt}$ information of the PA signal is not important, which can be neglected

$$A = K'\frac{\beta}{C_p}\frac{E_0\upsilon^3}{R^3\sqrt{r}}N_0\sigma_0 L(1 + KN_s), \tag{9}$$

where K' is a constant.

In Eq. (9), E_0, r, σ_0, σ_s, L, R are parameters independent with solute concentration. β, C_p, υ, N_w are related to the solute concentration, but are not highly affected by the concentration. For the detection of low-content substances, i.e. substances with Wt% less than 0.1%, the change of these parameters can be ignored. For example, when glucose concentration changes from 40 mg dl^{-1} to 1000 mg dl^{-1}, the acoustic velocity υ only changes from 1503.759 m s^{-1} to 1507.999 m s^{-1}.[25] For high-power pulsed lasers, it is difficult to control the laser energy per cycle, which means E_0 fluctuates greatly in the entire PA measurement and cannot be regarded as a constant. Finally, a much simpler expression is obtained as Eq. (10)

$$A = ME_0(1 + KN_s), \tag{10}$$

where $M = K'\frac{\beta}{C_p}\frac{\upsilon^3}{R^3\sqrt{r}}N_0\sigma_0$. The amplitude of the PA signal is linear with the concentration of the tested solute.

The amplitude A of PA signal is related to the solute concentration N_s and laser energy E_0 per circle. For high-power pulsed laser, E_0 is usually very unstable, resulting in inconsistent amplitudes of PA signals obtained from each measurement. In addition, in the measuring process, PA signals are easily affected by various environmental factors, such as environmental electromagnetic interference, ambient light fluctuation and temperature fluctuation. Single-cell PA measurement method has serious drawbacks such as high randomness and poor reproducibility, which cannot meet the measurement requirements.

Figure 1 demonstrates the setup of the experiment system. An 1064 nm Nd:YAG pulsed laser (STL1064QW-1 mJ, Stone Laser Co., Ltd., Beijing, China) was taken as the excitation source. The energy of a single-pulse laser was 0.5 mJ. The laser was modulated by a function generator (AFG310, Tektronix Japan, Ltd., Tokyo, Japan) and split by a beam splitter. The intensities of the two beams are adjusted by rotating a half-wave plate. The TPAC and RPAC were filled with the tested and reference solution. The two PA cells have same parameters. Solutions were added through a circulating drip system with an electric pump. Two temperature sensors with an accuracy of 0.01 °C were embedded in two PA cells to detect the solution temperature. Two identical water-immersion ultrasonic transducers (PZT-5A, 0.65 MHz center frequency, cylindrical with 25 mm diameter) were implemented to obtain PA signals. The distance between the detection surface of the two ultrasonic sensors and the center of laser energy was also identical, thus the change of the PA signal amplitude caused by the different detection distance can be avoided. A charge amplifier (HQA-15M-10T,

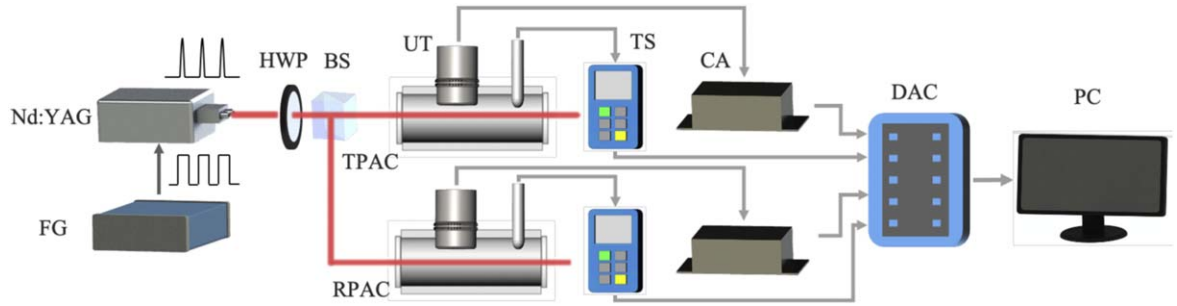

Fig. 1. (Color online) The experiment setup of the TCD-PA detection system. (FG: function generator, HWP: half wave plate, BS: beam splitter, TPAC: test PA cell, RPAC: reference PA cell, UT: ultrasonic transducer, TS: temperature sensor, CA: charge amplifier, DAC: data acquisition card).

FEMTO® Messtechnik GmbH, Schorndorf, Germany) with a gain of $10\,\mathrm{V\,pC^{-1}}$ was used to amplify PA signals, which were collected by a data acquisition card (DAC, Spectrum M2i.202, Bielefeld, Germany) with the sampling rate of $100\,\mathrm{MS\,s^{-1}}$ and then sent to a computer for processing.

Assuming the pulsed laser is split into two identical beams, the test solution and reference solution will receive the same laser energy with an amplitude of $E_0/2$ per cycle. With Eq. (10), the amplitude of the TPA signal and reference PA (RPA) signal is $A_t = ME_0(1 + KN_s)/2$ and $A_r = ME_0/2$, respectively. By calculating the ratio of A_t and A_r, the effects of laser intensity fluctuation and other multiplicative noise can be eliminated to obtain the concentration of the tested solute

$$N_s = \frac{1}{K}\left(\frac{A_t}{A_r} - 1\right). \tag{11}$$

However, the PA signal is not only related to the test substance concentration, but also parameters such as the volume expansivity and acoustic velocity. Although these parameters are not sensitive to the concentration of test substance, they are highly influenced by temperature. Changes in temperature have a direct impact on the substance sensing. Besides, in the differential PA measurement system, it is difficult to keep the temperature in two PA cells exactly the same. It is necessary to eliminate the influence of temperature on PA signals. When temperature T changes, the PA signal amplitude A varies linearly with the change.[32] The structural parameters of the two ultrasonic sensors and the PA cells are not completely consistent, resulting in different effective light intensity and inner temperature. To eliminate the error, the PA signal amplitude is firstly compensated by the TC model, then the adjusted PA amplitude A is used in Eq. (11) to further eliminate the effect of laser intensity fluctuation and other environmental interference.

Glucose was used as the test substance to demonstrate the effectiveness of the TCD-PA method for the detection of weakly absorbing substances. The concentrations of glucose solutions ranged from 0 to 690.0 mg $\mathrm{dl^{-1}}$, while the reference solution was distilled water deionized by a MilliQ Water System (18.2 MΩ . cm, Millipore CO., USA). Each concentration of the solution was repeatedly measured 10 times. During each test, the TPA and RPA signals, and the temperature of the TPAC and RPAC were acquired simultaneously. The intensity of the PA signal at each concentration was represented by peak-to-peak value (PPV) after 100 times averaging, as shown in Fig. 2(a). The experimental procedure of TCD-PA detection is shown in Fig. 3.

For each measurement, 1000 experimental results were equally divided into 10 groups. The relationship between the amplitude of the test PA (TPA) signal and glucose concentration is shown in Fig. 4(a), which shows no significant correlation.

Before TC, the PA temperature coefficient in two cells was obtained through experiments. Distilled water were heated to 40 °C using a water bath heating device, and then slowly injected into the TPAC and the RPAC respectively using a liquid pump. During natural cooling, the PA signals and temperature were recorded. The relationship between PA signal amplitude and solution temperature are shown in Fig. 2(b). Obviously, both the TPA signal and RPA signal rise linearly as the temperature increases. The solution temperature was fitted linearly to the PA signal amplitude, and the slope of the resulting fitted line was defined as the PA temperature coefficient. The obtained PA temperature coefficient of the TPAC, k_t, is 0.028 V $°C^{-1}$, and the PA temperature coefficient of the RPAC, k_r, is 0.025 V $°C^{-1}$.

After TC, the relationship between the glucose solution concentration and the TPA signal and the RPA signal

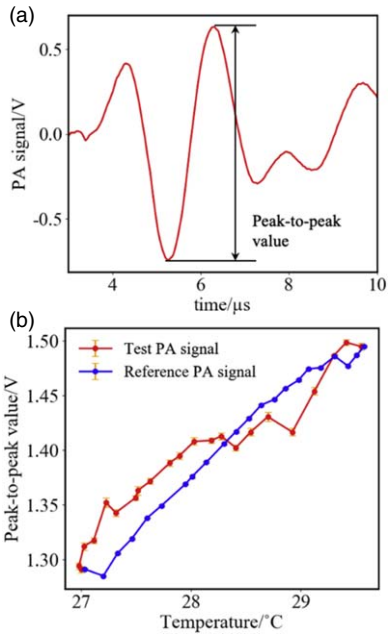

Fig. 2. (Color online) (a) A real PA signal and its peak-to-peak value as pointed by the black arrow), (b) The relationship between temperature and PPV of PA signal.

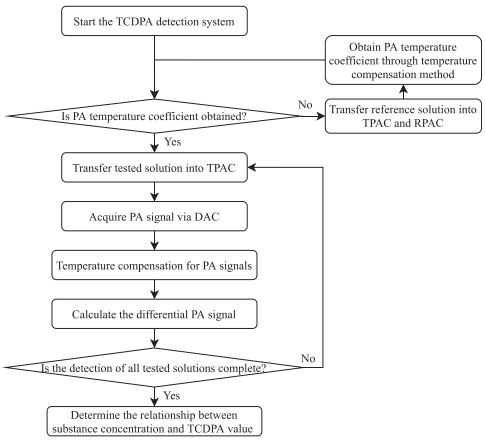

Fig. 3. A flow chart of TCD-PA detection procedure.

amplitude is shown in Fig. 4(c). From Eq. (10), the PA signal is positively correlated with glucose concentration. However, as shown in Fig. 4(c), there is no obvious correlation between the PPV after TC and the glucose concentration. The values still include the influence of other interference factors, such as laser intensity fluctuation, environmental noise, electromagnetic interference, etc.

To reduce the influence of inteferences, the TPA signal amplitude is divided by the RPA signal amplitude to obtain the differential PA value. The differential PA values without and with TC are shown in Fig. 4. Without TC, there is still no linear correlation between the differential PA values and the concentration. Therefore, it is necessary to combine TC and differential PA method to extract the content of weakly absorbing substances. The TCD-PA values rises linearly with glucose concentration ($R^2 = 0.973$). The feasibility of TCD-PA on weakly absorbing substances is confirmed theoretically and experimentally.

The detection accuracy of glucose concentration is also related to the laser wavelength. Although the difference between the absorption of glucose and water at 1064 nm is minimal, we still obtained a detection limit of 9.95 mg dl^{-1}. The detection limit can be further increased if a laser wavelength with stronger glucose absorption is chosen. If there are multiple substances in the solution, the content of the test substance can be extracted by a multi-wavelength PA detection method. However, this method cannot eliminate additive noise. When the concentration increases, the parameters such as viscosity and acoustic speed will change, resulting in the time profile change of the PA signal. The peak position will shift to the left. It is impossible to directly subtract the PA signal and RPA signal to reduce additive interferences.

The TCD-PA method effectively suppresses the influence of light intensity fluctuation, other multiplicative environmental noise and temperature fluctuation on the substance detection in liquid. The feasibility of this method is theoretically analyzed. A set of TCD-PA detection system was built to detect glucose solutions ranging from 0 to 690 mg dl^{-1} under 1064 nm. The corrected PA signal amplitude has a linear relationship with glucose concentration ($R^2 = 0.973$). By transferring liquid with an electrical pump and avoiding air bubbles and turbulence, this TCD-PA method can be used for monitoring liquid substance in trace-level.

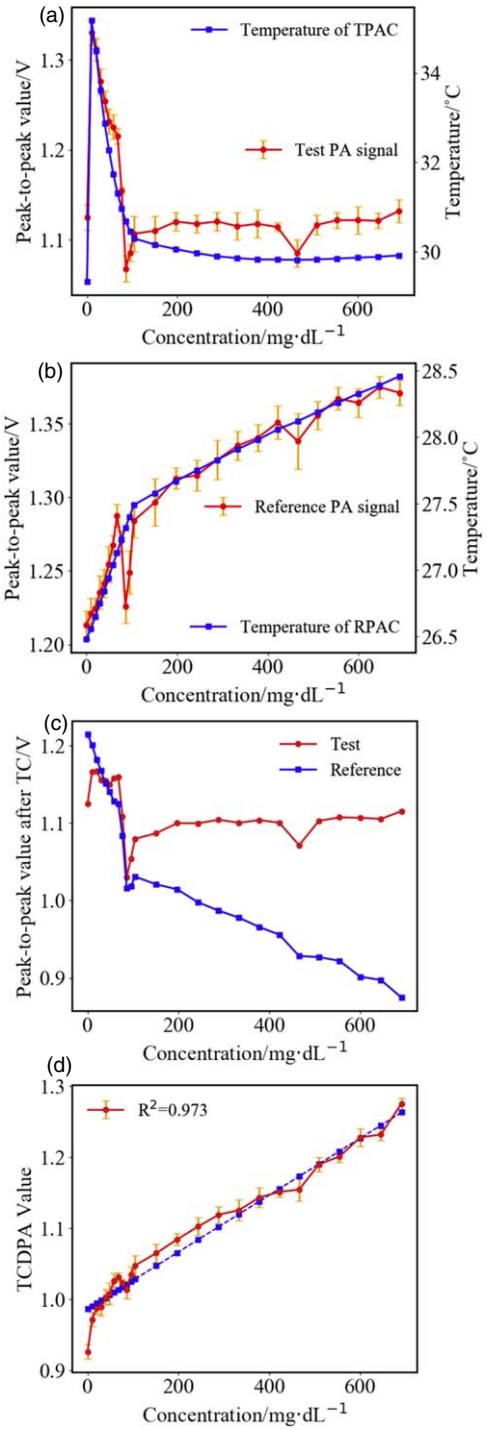

Fig. 4. (Color online) The experimental results of TCD-PA method. The PPV of (a) original test PA signals, (b) original reference PA signal, (c) tested and reference PA signal after TC, (d) PA signal obtained by the TCD-PA method.

Acknowledgments This work is supported by the National Natural Science Foundation of China under Grant No.61873168, which provides important financial conditions for this research.

ORCID iDs Qiaozhi He https://orcid.org/0000-0002-9475-8319

1) L. Ren, X. Zhang, X. Guo, H. Wang, and X. Wu, IEEE Photonics Technol. Lett. **29**, 639 (2017).
2) S. Panova, M. J. Cliff, P. Macek, M. Blackledge, M. R. Jensen, J. W. M. Nissink, K. J. Embrey, R. Davies, and J. P. Waltho, Structure **27**, 1537 (2019).
3) X. Yan, S. Dai, I. T. Graham, X. He, K. Shan, and X. Liu, Int. J. Coal Geol. **191**, 152 (2018).

4) Z. Qu, E. Steinvall, R. Ghorbani, and F. M. Schmidt, Anal. Chem. **88**, 3754 (2016).
5) M. B. Gumpu, S. Sethuraman, U. M. Krishnan, and J. B. B. Rayappan, Sens. Actuators B **213**, 515 (2019).
6) A. A. Ammann, J. Mass Spectrom. **42**, 419 (2007).
7) L. Yang, S. Tong, L. Zhou, Z. Hu, Z. Mester, and J. Meija, J. Anal. At. Spectrom. **33**, 1849 (2018).
8) E. M. Nolan and S. J. Lippard, Chem. Rev. **108**, 3443 (2008).
9) M. A. Bechlin, E. C. Ferreira, and J. A. G. Neto, Microchem. J. **132**, 130 (2017).
10) E. M. Carstea, J. Bridgeman, A. Baker, and D. M. Reynolds, Water Res. **95**, 205 (2016).
11) I. Maouli, A. Taguchi, Y. Saito, S. Kawata, and P. Verma, Appl. Phys. Express **8**, 032401 (2015).
12) S. Zhao, W. Tao, Q. He, H. Zhao, and H. Yang, Appl. Opt. **56**, 193 (2017).
13) B. Dong, C. Sun, and H. F. Zhang, IEEE. Trans. Biomed. Eng. **64**, 4 (2016).
14) J.-F. Li, C.-Y. Li, and R. F. Aroca, Chem. Soc. Rev. **46**, 3962 (2017).
15) R. Pandey, S. K. Paidi, T. A. Valdez, C. Zhang, N. Spegazzini, R. R. Dasari, and I. Barman, Acc. Chem. Res. **50**, 264 (2017).
16) C. Patel and A. Tam, Rev. Mod. Phys. **53**, 517 (1981).
17) A. Seki, K. Iwai, T. Katagiri, and Y. Matsuura, Appl. Phys. Express **10**, 072503 (2017).
18) A. Rosencwaig, Annu. Rev. Biophys. **9**, 31 (1980).
19) Q. He, Q. Zhang, W. Cao, T. Yin, S. Zhao, X. Yin, H. Zhao, and W. Tao, Microchem. J. **150**, 104058 (2019).
20) Y. Kong, J. Shen, and A. Fan, Anal. Sci. **33**, 925 (2017).
21) H. Wu, L. Dong, H. Zheng, Y. Yu, W. Ma, L. Zhang, W. Yin, L. Xiao, S. Jia, and F. K. Tittel, Nat. Commun. **8**, 1 (2017).
22) G. S. Kell, J. Chem. Eng. Data **20**, 97 (1975).
23) H. Coufal, R. Veith, P. Korpiun, and E. Lüscher, J. Appl. Phys. **41**, 5082 (1970).
24) Q. Zhang, J. Chang, Q. Wang, Z. Wang, F. Wang, and Z. Qin, Sensors **18**, 42 (2018).
25) S. Zhao, W. Tao, Q. He, H. Zhao, and W. Cao, AIP Adv. **7**, 035313 (2017).
26) F. H. Fisher and V. P. Simmons, J. Acoust. Soc. Am. **62**, 558 (1977).
27) J. Yang, L. Gong, X. Xu, P. Hai, Y. Shen, Y. Suzuki, and L. V. Wang, Nat. Commun. **8**, 1 (2017).
28) S. Manohar and D. Razansky, Adv. Opt. Photonics **8**, 586 (2016).
29) D. F. Swinehart, J. Chem. Educ. **39**, 333 (1962).
30) H. Lai and K. Young, J. Acoust. Soc. Am. **72**, 2000 (1982).
31) V. Del Grosso and C. Mader, J. Acoust. Soc. Am. **52**, 1442 (1972).
32) W. Tao, Z. Lu, Q. He, P. Lv, Q. Wang, and H. Zhao, Sensors **18**, 4323 (2018).